Application of Higher-Order Sliding Mode and Enhanced PI Controllers for Superior Harmonics Mitigation in Power Networks

Z. G. Usman*, O. Oghorada, O. Oshiga, B. Adetokun

Department of Electrical and Electronics Engineering, Nile University of Nigeria. Plot 681, Research & Institution Area, Airport Road, Jabi, Abuja.

ABSTRACT: Due to varying system parameters and fluctuating load conditions of power systems, classical control schemes are ineffective for controlling active power filters (APF). As such, this study proposed a combined application of an enhanced proportional-integral (EPI) and a higher-order sliding mode (HOSM) controllers in shunt active power filters (SAPFs). The controllers are applied in the SAPF in two schemes to test the viability of the control strategy under fluctuating load conditions. The choice of the EPI and HOSM is informed by the controllers' robustness to system parameter variations and external disturbances, which is crucial for SAPFs operating in dynamic load conditions. The results demonstrate that the adopted control strategy achieves good dynamic response, and a rapid voltage stabilization time of 0.1 seconds after $t > 0.4$ seconds. Furthermore, the total harmonic distortion (THD) is significantly reduced in the two schemes meeting the requirement set by IEEE – 519 standards for power quality in electrical networks. These findings highlight the robustness and efficacy of applying the adopted strategy in enhancing the performance of APFs, offering a promising solution for advanced harmonic mitigation and stable voltage control in modern power systems. Future research should focus on optimizing the computational aspects of the control strategy for real-time applications and further validating its effectiveness across diverse operational environments.

KEYWORDS: Harmonic currents, Higher-order sliding mode control, Power quality, Shunt active power filter

[Received Nov. 24, 2021; Revised May 15, 2022; Accepted May 26, 2022] Print ISSN: 0189-9546 | Online ISSN: 2437-2110

I. INTRODUCTION

The emergence of advanced technology for an array of applications has rendered the reliability of electrical power increasingly important. Power quality (PQ) is an expansive word that covers several difficulties that are related to electrical supply disruptions (Callegari et al. 2021). Poor PQ leads to severe consequences, including equipment overheating, malfunctioning of sensitive devices, and failure of electrical infrastructure, resulting in substantial economic losses (Deffaf et al. 2023).

In the past, classic methods for addressing PQ issues, particularly harmonics, relied on passive filters. These filters do not effectively remove all harmonics from the electrical system since they only suppress selected tuned harmonics (Buła et al. 2022). They have the drawback of being greater in size and weight, as well as producing undesirable resonances. Active Power Filters (APF) efficiently overcome the inadequacies of passive power filters (Callegari et al. 2021; Musa et al., 2014). APFs can correct for reactive power, voltage, and current harmonics, enable voltage control in distribution infrastructure, and eventually assist in lowering financial losses in the system. Shunt APFs inject equal but opposite-phase compensation currents to eliminate the harmonic currents and reactive components at the point of common coupling (PCC) (Wang et al. 2018). Despite their advantages, the performance and operational efficiency of APFs are heavily dependent on the control strategies employed (Naftahi et al. 2022; Rashid, 2017). A shunt APF consists of a 3-phase electronic power converter, which is connected in parallel to the power source to provide compensating currents for the voltage source inverter (VSI). To achieve the correct output currents, a control system must give the appropriate trigger pulses to switch the ON/OFF states of the converter's electronics system (Hoon et al. 2016). The current controller is referred to as the nerve centre of the APF since it generates PWM switching pulses for the voltage source inverter. Normally, this algorithm is designed to generate compensation currents under specified harmonic reference current signals (Puhan et al. 2021a).

Researchers have investigated several control techniques to mitigate harmonics in power systems. Sozanski and Szczesniak, (2023) presented a digital control algorithm for a three-phase APF shunt utilizing a switching-sliding discrete Fourier transform to address long-term stability issues inherent in traditional first harmonic detector circuits using the classical sliding discrete Fourier transform algorithm. The proposed switching-sliding discrete Fourier transform algorithm operates two sliding discrete Fourier transform algorithms in parallel, consecutively resetting them to eliminate numerical errors and significantly improve stability, with only a 25% increase in arithmetic operations. The approach was validated

*Corresponding author: zubairugats@gmail.com

doi: http://dx.doi.org/10.4314/njtd.v22i1.2786

through experimental tests using the TMS320F28379D microcontroller, demonstrating a significant reduction in numerical errors and effective APF control. Ben Abdelkader et al. (2023) proposed a synergetic control using a phase-locked loop technique for a 3-phase 3-level clamped VSI-based SAPF to compensate for harmonics, thus improving power quality in electrical distribution networks. This control strategy does not require solving state equations or knowing system poles, it controls the DC voltage and active filter currents, and its efficiency was verified through MATLAB/Simulink simulations for RL and RC load scenarios. The simulation results showed that the control strategy significantly outperforms traditional control methods in reducing harmonics and producing fast dynamic response, highlighting its effectiveness and robustness. Naftahi et al. (2022) introduce a hybrid automaton approach with instantaneous reactive power theory for a three-phase, four-wire shunt APF employing a three-leg split capacitor VSI. The method compensates for undesired harmonic, reactive currents from nonlinear loads and regulates the DC link capacitor voltage, achieved through a two-loop cascaded controller where the inner loop ensures unity power factor using the hybrid automaton approach. The outer loop uses a proportional-integral (PI) regulator for precise DC bus voltage regulation. The simulation software MATLAB/SimPowerSystems validates the theoretical results, demonstrating the controller's effectiveness in achieving power factor correction and stable DC voltage regulation.

Musa et al. (2017) explore a shunt APF as a complete current source solution for eliminating harmonic currents in a power system, focusing on its reference current generation strategy, control technique, and inverter topology. The authors implemented a fuzzy logic current control technique to generate pulse width modulation pulses for a three-phase inverter and used a bandpass filter in the synchronous reference frame algorithm for harmonic extraction. The performance of the shunt APF was evaluated using MATLAB/Simulink under balanced voltage conditions, showing effective and satisfactory harmonic mitigation. Wang et al. (2018b), improved APF efficiency by analysing the influence of DC link voltage on the APF's compensating current and performance, emphasizing the need to maintain the DC-link voltage at a minimum value. The simplified minimum DC-link voltage control strategy was proposed, which regulates the voltage solely on grid voltage and modulation ratio, reducing computational complexity and implementation difficulty while avoiding external interference. Investigational outcomes from a shunt APF prototype validated the effectiveness and correctness of the proposed strategy, demonstrating its potential for efficient harmonic elimination in power systems. Hoon et al. (2016) examined a new control technique called inverted error deviation control. This technique was integrated into the main DC-link capacitor voltage regulation algorithm of a SAPF to enhance overall DC-link voltage regulation. The control technique addresses the inadequacies of conventional proportional-integral (PI) and fuzzy logic control algorithms. The results were simulated in MATLAB/Simulink and validated using a TMS320F28335 digital signal processor, showing superior accuracy and dynamic response compared to the classic PI and fuzzy logic control methods.

Controlling Active Power Filters (APFs) is a complex task that demands precise filter output regulation to effectively mitigate harmonics, compensate reactive power, and regulate DC bus voltage (Divyalakshmi and Subramaniam, 2017). While traditional control strategies like Proportional-Integral (PI) controllers are commonly used, they have inherent limitations, including sensitivity to parameter variations and inability to handle non-linearities or dynamic loads. To overcome these challenges, researchers have delved into advanced control techniques, including Sliding Mode Control (SMC). However, the effects of using an enhanced PI voltage controller with a higher-order sliding mode current controller on shunt APFs have not been examined.

The Sliding Mode Control (SMC) is a robust current control strategy that offers several advantages, including insensitivity to parameter variations, disturbance rejection, and strong robustness against non-linearities. SMC drives the system's state trajectory onto a predefined sliding surface and maintains it there, ensuring the desired dynamic performance (Komurcugil et al., 2021). Nevertheless, conventional SMC techniques suffer from chattering, a phenomenon characterized by high-frequency oscillations that lead to wear and tear of the system components (G Bartolini, 1998). This drawback coupled with other inefficiencies, makes the SMC incapable of producing effective harmonics mitigation in APFs. The HOSM control strategy has been developed to address this issue.

Incorporating higher-order derivatives of the sliding surface effectively reduces chattering while preserving the robustness and disturbance rejection properties of SMC. The higher-order sliding mode (HOSM) control has demonstrated significant potential across various applications. This paper presents an approach that integrates the HOSM controller with an enhanced proportional integral (EPI) controller for Shunt APF to enhance power quality. The EPI controller is used to regulate the DC bus voltage, ensuring that it remains stable and within the desired limits. Meanwhile, the HOSM control is responsible for current control to generate pulse signals for the voltage source inverter, ensuring that harmonic currents are effectively cancelled out. This combination leverages the strengths of both control strategies: the simplicity and steady-state accuracy of the EPI controller, and the robustness and dynamic performance of the HOSM control strategy. The result is an effective control system for APFs that outperforms traditional methods. This novel combination is tested in multiple scenarios with diode and thyristor nonlinear loads to verify the robustness of the controllers to dynamic load changes. The consequences and positive effects of adopting a combination of the EPI and HOSM control strategy in SAPFs have not yet been investigated. Thus, this research contributes to the advancement of robust control techniques in shunt APFs as follows:

1. Developing robust control techniques for efficient DC voltage regulation and switching current control in SAPFs.

2. Significant reduction of Total Harmonic Distortion (THD) to levels below the IEEE-519 regulation standards and improvement of power factor through the integration of the EPI and HOSM controllers.

3. Achieving a 65% improvement in THD for diode non-linear loads with the developed controller compared to the results reported in (Amini et al., 2024).

Based on these contributions, the study intends to highlight the effectiveness of combining the EPI and HOSM control strategy applied and tested in various scenarios under dynamic load conditions. The rest of the study is arranged as follows. Section 2 describes the theoretical analysis and Section 3 presents modelling and simulation of the HOSM and EPI controllers for harmonics mitigation. Section 4 presents the results and discussion and then Section 5 concludes the study.

II. THEORETICAL ANALYSIS

A. System Description

The shunt APF in Figure 1 is physically connected to the electrical network in parallel at the point of common coupling. Nonlinear loads comprising two diode RL loads are implemented separately in the two schemes used for this research. The beneficial features of this proposed system include simplicity, ease of regulation, application, and maintenance. There are fundamentally two approaches to compensate for harmonics in electrical networks using APFs. The first stage identifies the harmonic components of the currents, which are subsequently introduced into the electrical network in phase opposition during the second stage.

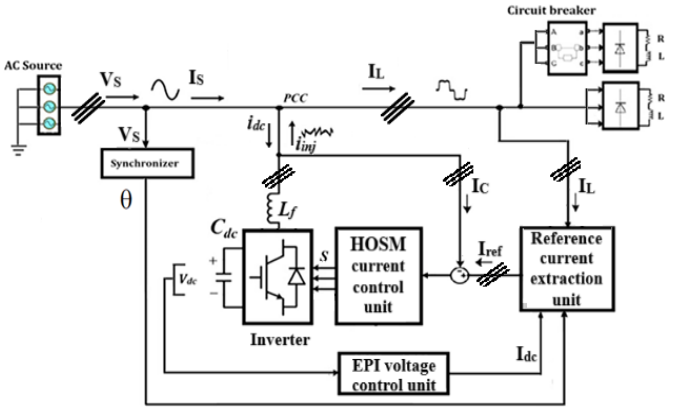

Fig. 1 Shunt APF model with the control units

Assuming that the shunt APF in Figure 1 is not connected to the grid, the flow of current in a contaminated power system is mathematically expressed as (Hoon et al. 2017):

$$I_S = I_L = I_{fd} + I_H \quad (1)$$

Where I_S denotes the source current, I_L load current, I_{fd} the fundamental current, and I_H is the harmonic current in the polluted power system. The source current from equation 1 is literally distorted due to the addition of harmonic currents (I_H) in the system.

The shunt APF parameters adopted for the study are shown in Table 1. The shunt APF system is connected to a 3-phase, 3-wire AC system with a 50 Hz frequency.

Table 1. The shunt APF System Parameters

Parameter Description	Values
Fundamental frequency	50 Hz
Source voltage/Phase	220V
Converter (Full bridge VSI)	3 phase, 3 legs
Switches type	IGBT
Source impedance (Rs, Ls)	0.15Ω, 0.03mH
Line impedance (Rr, Lr)	1Ω, 1mH
Nonlinear load (R_L,L_L)	10Ω, 2mH
Filter inductance	1mH
DC Voltage	300V
DC bus Capacitance (CDC)	2200μF
Low pass filter (f_o)	7Hz
Quality factor (Q)	1.4
Bandwidth (BW)	10

B. The Active Power Filter (APF)

Active Power Filters (APF) efficiently overcome the inadequacies of passive power filters which can only respond to specific harmonic frequencies in mitigating harmonic distortions in power systems. The APF is an effective tool for addressing power quality issues under dynamic load conditions in power networks. Furthermore, it has various advantages, including greater filtering accuracy, higher dynamic responsiveness, modularity, and flexibility, making it an ideal device for harmonic compensation and power quality improvement (Buła et al. 2022). APFs can correct for reactive power, voltage, and current harmonics, regulate voltage in distribution networks, and ultimately assist in reducing financial losses for both service providers and customers. Active power filters can perform functions other than harmonic reduction, such as power factor correction. In most ideal circumstances, harmonic-producing non-linear loads are made up of a mixture of harmonic currents, voltages, and unbalanced loads (Wang et al. 2018). APFs are used in power systems to address numerous power quality issues. They are primarily coupled in series, parallel, mix of series and parallel APFs, and a combination of active and passive power filters to produce a hybrid filter (Callegari et al. 2021; Deffaf et al. 2023).

C. Higher-Order Sliding Mode Control

The sliding mode control (SMC) is a robust nonlinear control strategy that is commonly utilized in engineering applications, especially for structures having uncertainties or external perturbations or disturbances. This control technique alters the behaviour of a nonlinear system by employing discontinuous adjustments and controls. The SMC method is effective for producing switching signals for voltage source inverters in nonlinear systems. It involves bringing the system's state trajectory onto a user-defined sliding surface and maintaining it there for the duration of the control period. The inefficiencies of the conventional SMC usually result in the generation of a reasonable amount of losses (Benbouhenni, 2019). Although the SMC strategy is simple to implement, it necessitates the application of discontinuous control rules, which can cause high-frequency oscillations of the variable under control. This phenomenon is known as chattering. Several approaches to reducing the chattering have been

proposed in the literature, including boundary layer control and filtered control. However, in these instances, the resilience and robustness of the SMC control could be lost. According to Cucuzzella et al. (2015 the chattering phenomenon can effectively be eliminated by increasing the order of the sliding mode. The higher-order sliding mode (HOSM) technique is deliberately designed with the increased order to eliminate the chattering phenomenon and increase the entire system's efficiency. During the filtering process, current regulation is achieved which produces the required switching pulses, enabling the shunt APF to function as an efficient compensator (Rahman et al. 2020). The HOSMC can be created in two steps. In the first step, an appropriate sliding surface is created and in the second step, a control law is generated to compel the system trajectories to reach the sliding surface and remain there (Zenteno-Torres et al. 2021). The discontinuous part takes the system onto a sliding surface. Once the system reaches the sliding surface, the continuous part (equivalent law) guarantees that the system remains there (Vargas-Gil et al. 2017).

D. Enhanced PI (EPI) control technique

Traditionally, PI controllers are developed using a linearised model at equilibrium. Yet, this linearization fails to account for uncertainties that could result in large transients that harm the operation of electrical equipment and power converters' signal output (Ahmed et al. 2018; Vargas-Gil et al. 2017). Conventional PI controllers are commonly utilized because they are simple to manage in controlling the DC bus voltage of shunt APFs. However, they have significant limitations, particularly when dealing with complex and dynamic systems such as APFs operating under unstable and dynamic load conditions (Karafotis et al. 2020). Furthermore, PI controllers do not respond rapidly to changes in variable load conditions. This can cause a continual divergence from the acceptable DC bus voltage boundary (Panda and Patel, 2015). To circumvent these constraints and limitations, sophisticated control methods are implemented to enhance the PI controller and improve its ability to respond to dynamic changes more efficiently.

Shunt APF losses represent the active power that the system must inject into the DC capacitor C_{dc} to maintain a stable voltage. Shunt APF losses principally include switching losses of the inverter circuitry like diodes and IGBTs (dos Santos Alonso et al., 2020). The EPI maintains a constant and stable voltage under dynamic loads enabling the shunt APF to carry out the compensation process more effectively. Maintaining a stable voltage across the DC-link capacitor is critical, and it should be maintained at a level sufficiently high so that the shunt APF can sufficiently produce the required injection currents $\boldsymbol{i_{inj}}$ directly back into the polluted power network. When the switching losses in shunt APF equals the true power used by the filter, the harmonics mitigation procedure is considered to be complete (Wang et al. 2015; Zafar et al. 2018).

E. Reference Current Extraction algorithm

Several control methods for extracting reference currents from distorted load currents have been discussed in various literature. Such extraction techniques can be applied in the time or frequency domains. The APF injects equal but opposite-phase compensating currents to reduce harmonic currents and reactive elements at the PCC (dos Santos Alonso et al., 2020; Li et al., 2021). The Modified Synchronous Reference Frame (MSRF) approach is used to extract harmonics and produce reference signals. The technique relies on the SRF methodology and uses a compact unit vector circuit to synchronize the system (Musa et al., 2017), a DC bus capacitor for voltage control, and stationary as well as rotating frames to extract harmonic currents. The most important component of this technique is that the voltage imbalance does not affect the generation of reference signals, hence improving resilience and efficiency of the process (Donghua Chen, 2004).

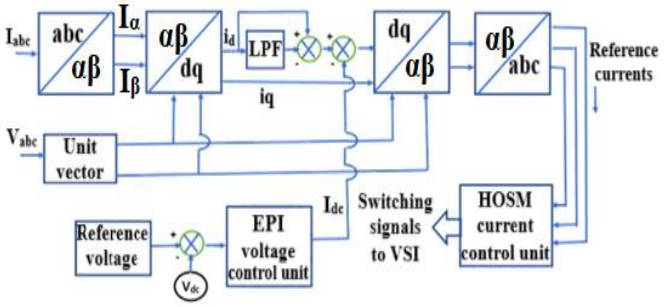

Fig. 2 Block diagram of the modified SRF method (Musa et al. 2017)

Figure 2 explicitly describes the transformation processes of the Modified Synchronous Reference Frame method (Musa et al., 2017). The a-b-c coordinates are converted into α – β coordinates in equation 2.

$$\begin{bmatrix} i_\alpha \\ i_\beta \end{bmatrix} = \sqrt{\frac{2}{3}} \begin{bmatrix} 1 & -\frac{1}{2} & \frac{1}{2} \\ 0 & \frac{\sqrt{3}}{2} & -\frac{\sqrt{3}}{2} \end{bmatrix} \cdot \begin{bmatrix} i_a \\ i_b \\ i_c \end{bmatrix} \quad (2)$$

Here, a unit vector instead of a PLL is used to generate sine and cosine signals that are synchronized with the relevant currents and voltages to transition from α − β plane to a d-q rotating frame. The current expression in the d-q axis is provided in equation 3;

$$\begin{bmatrix} i_d \\ i_q \end{bmatrix} = \begin{bmatrix} \sin(\theta) & -cos(\theta) \\ cos(\theta) & sin(\theta) \end{bmatrix} \cdot \begin{bmatrix} i_\alpha \\ i_\beta \end{bmatrix} \quad (3)$$

Where θ is the phase angle of voltage, i_α and i_β represent currents in the α – β frame.

An LP filter is used to change all the harmonics with DC values to non-DC quantities at correctly chosen frequencies as shown in equation 4:

$$\begin{bmatrix} i_d \\ i_q \end{bmatrix} = \begin{bmatrix} \bar{\imath}_d + \tilde{\imath}_d \\ \bar{\imath}_q + \tilde{\imath}_q \end{bmatrix} \quad (4)$$

Where $\bar{\imath}_d$ *and* $\tilde{\imath}_d$ represent the fundamental and harmonic component of d - frame load current while $\bar{\imath}_q$ *and* $\tilde{\imath}_q$ holds for fundamental and harmonic currents in q – frame.

Thus, i_α and i_β are obtained in equation 5:

$$\begin{bmatrix} i_\alpha \\ i_\beta \end{bmatrix} = \begin{bmatrix} sin(\theta) & -cos(\theta) \\ cos(\theta) & sin(\theta) \end{bmatrix}^{-1} \begin{bmatrix} \tilde{\imath}_d \\ \tilde{\imath}_q \end{bmatrix} \rightarrow$$

$$\begin{bmatrix} i_\alpha \\ i_\beta \end{bmatrix} = \begin{bmatrix} sin(\theta) & cos(\theta) \\ -cos(\theta) & sin(\theta) \end{bmatrix} \cdot \begin{bmatrix} \tilde{\imath}_d \\ \tilde{\imath}_q \end{bmatrix} \quad (5)$$

Equation 6 gives the reference currents $i_{\alpha\text{-ref}}$ and $i_{\beta\text{-ref}}$

$$\begin{bmatrix} i_{\alpha-ref} \\ i_{\beta-ref} \end{bmatrix} = \begin{bmatrix} sin(\theta) & cos(\theta) \\ -cos(\theta) & sin(\theta) \end{bmatrix} \cdot \begin{bmatrix} \widetilde{i_d} + i_{dc} \\ \widetilde{i_q} \end{bmatrix} \quad (6)$$

Lastly, in *ABC* frame, the reference currents are given thus:

$$\begin{bmatrix} i_{a-ref} \\ i_{b-ref} \\ i_{c-ref} \end{bmatrix} = \sqrt{\frac{2}{3}} \begin{bmatrix} 1 & 0 \\ -\frac{1}{2} & \frac{\sqrt{3}}{2} \\ \frac{1}{2} & -\frac{\sqrt{3}}{2} \end{bmatrix} \cdot \begin{bmatrix} i_{\alpha-ref} \\ i_{\beta-ref} \end{bmatrix} \quad (7)$$

These extracted reference currents in equation 7 are measured against inverter currents and used to generate switching signals (S) for the inverter.

III. MODELING AND STIMULATION OF THE HOSM AND EPI CONTROLLERS FOR HARMONICS MITIGATION

This section employs the control strategies of the shunt active power filter for effective harmonics mitigation. The efficiency of shunt APFs usually depends on the control strategies employed during the compensation process.

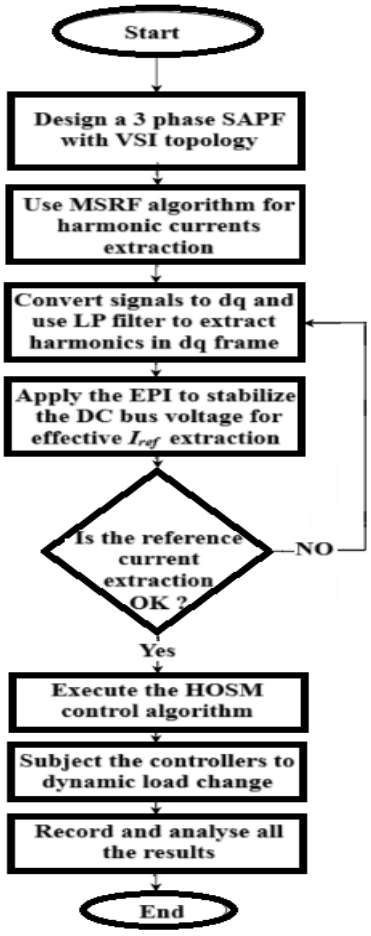

Fig. 3 Flowchart showing the SAPF's compensation process

The various stages involved in the compensation process is illustrated in the flowchart shown in Figure 3. Advanced SAPF control strategies employed in this research provide better performance compared to the conventional approaches like PI and sliding mode control.

A. *Enhanced PI control strategy*

As an advanced voltage regulator, the EPI controller in Figure 4 generates the required reference current I_{dc} for stabilizing the system's voltage to align with its reference V^*_{dc} value of 300 volts. The eight gains of the EPI voltage controller are tuned to the desired state in order to obtain the optimal solution.

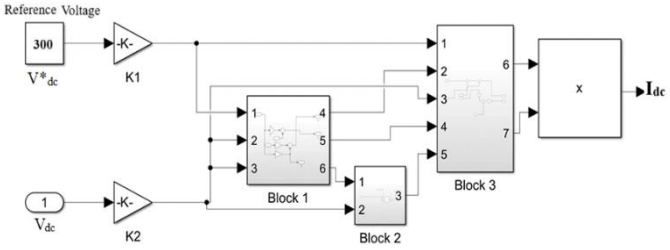

Fig. 4 Enhanced PI voltage controller

Figures 5, 6, and 7 demonstrate how the three blocks shown in Figure 4 are interconnected.

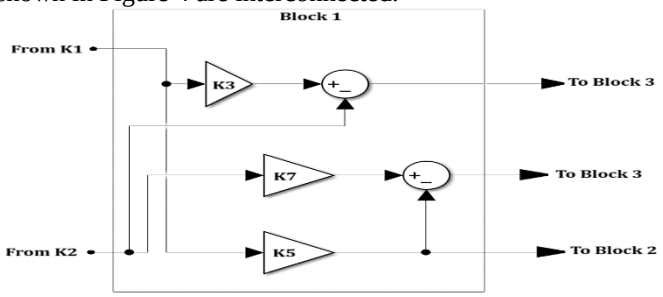

Fig. 5 Internal circuitry of block 1

The error signal required to maintain the DC bus voltage at the desired value is given as;

$$e = V_{dc} - V^*_{dc} \quad (8)$$

From Figure 5;

$$V^*_{dc}K_1K_3 - V_{dc}K_2 \quad (9)$$

$$V_{dc}K_2K_7 - V^*_{dc}K_1K_5 \quad (10)$$

The relational operator in Figure 6 is crucial for the decision-making and control process in the EPI controller. It compares the Vdc values from K2 with the output of block 1 and provides an appropriate signal going into block 3.

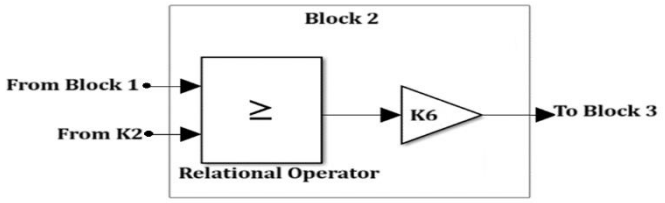

Fig. 6 Internal circuitry of block 2

From Figure 6;

$$(V_{dc}K_2 \geq V^*_{dc}K_1K_5)K_6 \quad (11)$$

The integral shown in Figure 7 guarantees stability by combating persistent disturbances under dynamic load conditions that create variations in system responsiveness, resulting in voltage drift over an extended period.

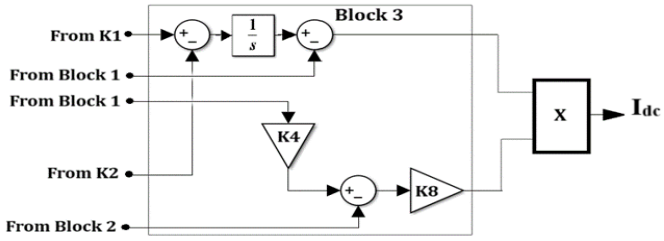

Fig. 7 Internal circuitry of block 3

From Figure 7, the output of the enhanced PI controller is given as;

$$\int [V_{dc}^{*} K_3 K_1 - V_{dc} K_2] - (V_{dc} K_2 K_7 - V_{dc}^{*} K_5 K_1) \quad (12)$$

$$[-V_{dc}^{*} K_1 K_5 K_6 + (V_{dc}^{*} K_1 K_3 - V_{dc} K_2) K_4] K_8 \quad (13)$$

Therefore;

$$I_{dc} = (\int [V_{dc}^{*} K_1 (1 - K_5) - V_{dc} K_2 (1 - K_7)]) (V_{dc}^{*} K_1 (K_3 K_4 - K_5 K_6) - V_{dc} K_2 K_4) K_8 \quad (14)$$

$V_{dc}\, K_2 \geq V_{dc}^{*} K_1\, K_5$

Where;

$K_n > 0, \quad and\ n = 1 \cdots 8$

The optimum performance of the controller is achieved when the values of gains K1 to K8 are greater than zero as shown in Table 2.

Table 2. Optimum values of the gains in the controllers

Controller	Gain	Optimum value
	K1 = K2	0.12
	K3	1.0
EPI	K4	0.19
	K5	2.0
	K6	0.0000059
	K7	1.009
	K8	0.433
	K_u	0.1
HOSM	K_w	0.25

B. Higher-Order Sliding Mode Control Strategy

These algorithms operate by comparing the actual current to the reference current in dq frames as shown in Figure 8. The desired compensation current is created based on the error that was discovered by the controller.

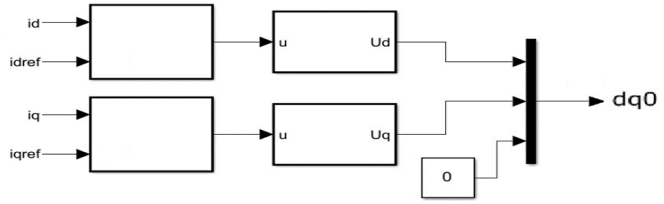

Fig. 8 Conversion of the currents into dq0 frames

The control algorithm shown in Figure 9 produces the appropriate switching pulses, as well as an internal current control cycle which guarantees that the compensation current (I_C) is generated by the reference currents. By introducing the I_C into the power network, the waveform of the grid current is adjusted, completing the shunt APF's compensating process.

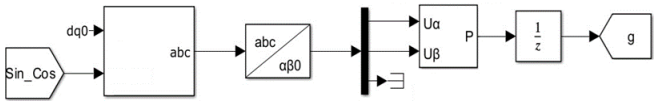

Fig. 9 Generation of switching currents for the VSI

C) Sliding Surface Design

For the SAPF, modulating signal U is basically regarded as the control input. While creating the sliding mode controller, control input can be composed of two parts, a continuous part U_{eq} and the discontinuous part U_n as shown in Equation 15

$$U = U_{eq} + U_n \quad (15)$$

In the d-q frame, the control can be expressed by Equation 16

$$U_{dq} = U_{eq,dq} + U_{n,dq} \quad (16)$$

Therefore, the sliding surface σ_i is defined as;

$$e = i_{i,f} - i_{i,ref}$$

$$\sigma_i = \ddot{e} + k_2 \dot{e} + k_1 e \quad (17)$$

Where σ_i is the sliding surface, e is the error, k_1 and k_2 are tuning parameters, $i = d, q$, $i_{i,ref}$ is the reference current and $i_{i,f}$ represents the compensating current.

The sliding surface is used to formulate the control law in (18).

$$U_i = -K_{u,i} \sqrt{|\sigma_i|}\, sign(\sigma_i) - K_{w,i}\, sign(\sigma_i) \quad (18)$$

Where $sign(\sigma_i)$ is termed the discontinuous law and is given as;

$$sign(\sigma_i) = \frac{\sigma_i}{abs(\sigma_i)}$$

$$K_{u,i}, K_{w,i} > 0, \quad (19)$$

The control limits of the circuit are - 1 ≤ U_i ≤ 1, this expression can be used for the equivalent

control for both a design procedure, and to establish the performance of the filter. Therefore σ_i can be expressed as;

$$\sigma_i = \begin{cases} 1 & sign(\sigma_i) > 0 \\ -1 & sign(\sigma_i) < 0 \end{cases} \quad (20)$$

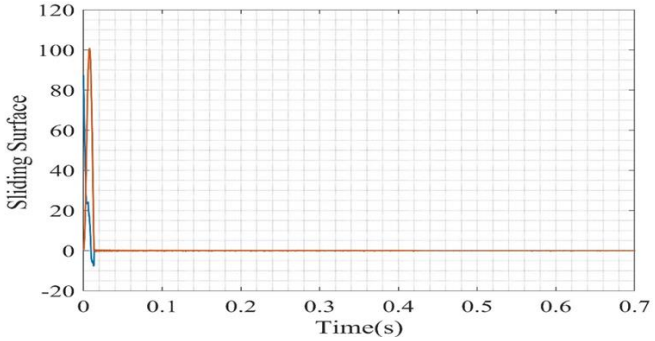

Fig. 10 Sliding surface achieved with the HOSM control technique

From Figure 10 it can be observed that the higher-order sliding mode control implemented was able to force the system trajectories to reach the sliding surface and stay there. This result demonstrates the robustness of the proposed control technique in mitigating harmonics and eliminating the chattering phenomenon.

D) Stability Analysis of the System

The Lyapunov function is given as;

$$V = \frac{1}{2}\sigma_i^2 \quad (21)$$

Taking the derivative of equation (21)

$$\dot{V} = \sigma_i \dot{\sigma_\iota} \quad (22)$$

For the system to be stable,

$$\sigma_i \dot{\sigma_\iota} < 0 \quad (23)$$

Let $\dot{\iota_{,f}} - \dot{\iota_{,ref}} = K_{u,i}\sqrt{|\sigma_i|}sign(\sigma_i) + K_{w,i}sign(\sigma_i)$

$\sigma_i \dot{\sigma_\iota} = \sigma_i(K_{u,i}\sqrt{|\sigma_i|}sign(\sigma_i) + K_{w,i}sign(\sigma_i) + K_{u,i}\sigma_i - K_{u,i}\sigma_i)$

$\dot{V} = -K_{u,i}\sigma_i^2 + \sigma_i(K_{u,i}\sqrt{|\sigma_i|}sign(\sigma_i) + K_{w,i}sign(\sigma_i) + K_{u,i}\sigma_i)$ (24)

From equation (17), the system will remain stable when, $\dot{V} < 0$,

$$\therefore U_i = -K_{u,i}\sqrt{|\sigma_i|}sign(\sigma_i) - K_{w,i}sign(\sigma_i) - K_{u,i}\sigma_i$$

IV. RESULTS AND DISCUSSION

The main findings obtained using MATLAB/Simulink software R2022b for the shunt APF in Figure 1 are discussed and analysed here. The main objective is to investigate the robustness and viability of the controllers under dynamic load conditions in multiple scenarios. The simulation results are analysed for two schemes in this research:

A. *Thyristor rectifiers simulated using firing angles of 5°, 30°, and 60° and*
B. *Diode bridge rectifiers with RL loads using the same parameters as (Amini et al., 2024).*

The performance of the adopted controllers was compared with the controller used in (Amini et al., 2024). The results are tabulated and analysed extensively.

***A. Scheme 1**: Thyristor rectifier nonlinear load*

Simulation tests were conducted on the SAPF with thyristor rectifiers at various firing angles, using the higher-order sliding mode current control strategy. At t = 0.4 s, a load change was induced to test the robustness of the proposed controller in responding to dynamic load conditions. Before compensation, the load current (phase a) waveform shown in Figure 11 is distorted by the harmonics injected by nonlinear loads in the power system. After compensation with a shunt APF, the distorted current (phase a) waveforms become sinusoidal and in phase with the source voltage as shown in Figure 12. It can be noted that before or after the load changes, the APF appropriately tracks its reference, ensuring a sinusoidal waveform for the source current.

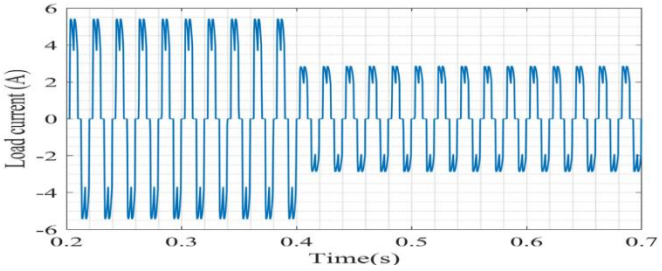

Fig. 11 Load current waveform before compensation

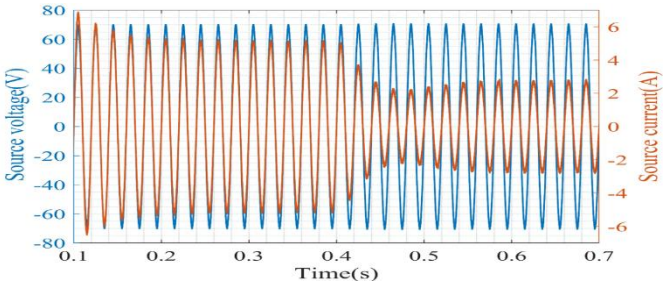

Fig. 12 Source current and voltage waveforms after compensation

Harmonic spectrums illustrated in Figure 13 obviously indicate that the proposed control permits fewer THDs under IEEE 519 regulations for harmonics in power systems. From Figure 13 it can be observed that the THD on the source current is reduced from 32.29% before compensation to 2.21% after compensation at a firing angle of 5°. The THD values were slightly reduced to 2.20% when the firing angles were changed to 30° and 60°, respectively, as shown in Figure 14. The proposed strategy reduced the THD values by about 93% during the dynamic test, irrespective of the thyristor firing angle. This outcome demonstrates the controller's fast response to dynamic load changes. It also demonstrates the ability of the proposed technique in mitigating complex harmonics and elimination of system imbalance in power networks.

The effectiveness of this technique is clearer in Figure 15 which shows a faster response to sudden changes in the load. It is clear that the dynamic performance of the adopted strategy is exceptionally good. The results indicate that the DC bus voltage regulation is performed with a faster reaction. It produced a much smaller overshoot during load changes, resulting in sustained DC voltage stability.

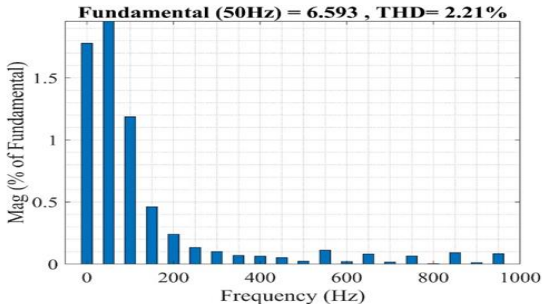

Fig. 13. THD produced using the proposed controller with a thyristor rectifier at firing angle 5°

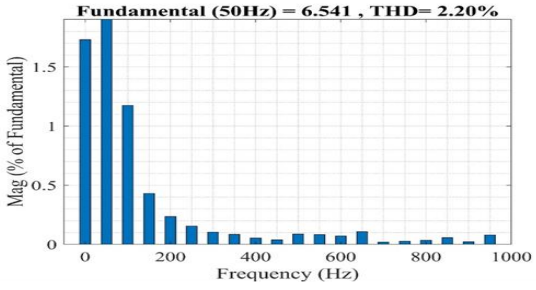

Fig. 14. THD produced using the proposed controller with a thyristor rectifier at firing angles 30° and 60°

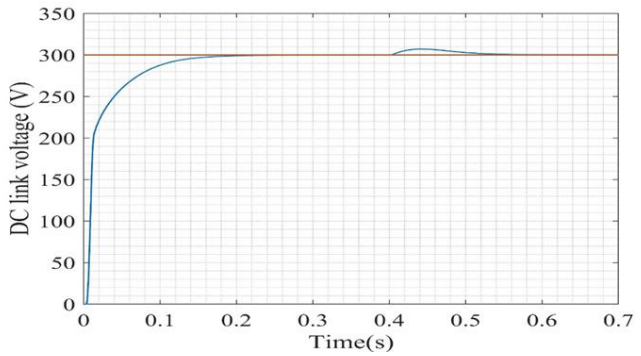

Fig. 15 DC voltage profile for the thyristor rectifier nonlinear loads

B. *Scheme 2: Diode bridge rectifier with RL load*

To evaluate the reliability of the proposed controllers for harmonics mitigation, their performance was compared to that of (Amini et al., 2024) using the same parameters in a shunt APF model. Simulations were carried out using the HOSM technique with a diode bridge rectifier connected to an RL load, as shown in Figure 1. At time t = 0.4 s, a load change was introduced. The voltage and current waveforms obtained indicate a similar outcome to that obtained with the thyristor rectifier nonlinear load. The SAPF current precisely tracks its reference during the dynamic test, resulting in a smooth sinusoidal waveform for the source current with a better power factor.

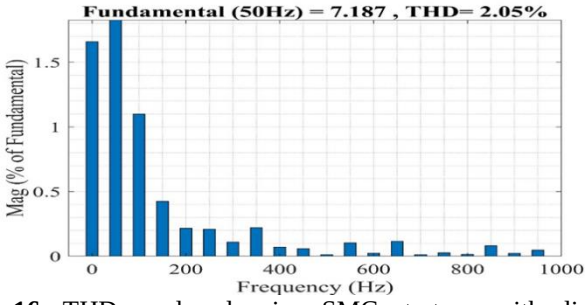

Fig. 16. THD produced using SMC strategy with diode rectifier nonlinear RL load

Harmonic spectrums of the source current with the HOSM controller are presented in Figure 16. After the filtering, it is clear that the current control technique significantly reduces the harmonic content of the source current, from 27.45% to 2.05%.

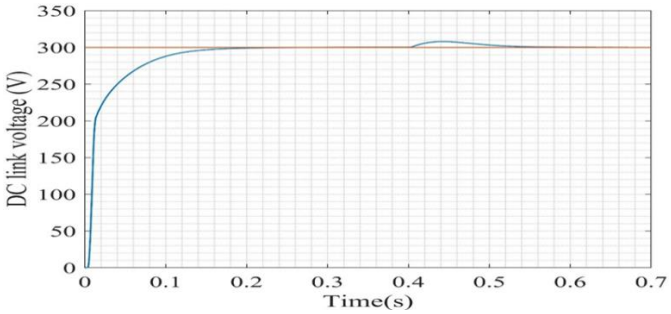

Fig. 17 DC voltage profile for the thyristor rectifier nonlinear loads

Figure 17 displays the DC voltage profile under RL load. This control technique achieves faster response and prevents an overshoot when t < 0.4 s, resulting in stable DC bus voltage.

Additionally, the voltage profile in Figure 17 indicates good stability and minimal DC bus voltage (Vdc) vibrations during a steady State Period. The controller's robustness to changes in the load were demonstrated by the fast return to the reference track change when t > 0.4 s.

In Table 3, the main comparative results between the suggested control strategy and the Proportional-Resonant (PR) controller implemented by (Amini et al., 2024) were summarized. The proposed strategy eliminated the overshoot of the DC bus voltage when t < 0.4 s. Furthermore, undershoot of DC bus voltage was literally eradicated during the dynamic test paving the way for a smooth and stable shunt APF system operation. The recorded results confirm the superiority of the suggested control technique in mitigating complex harmonics under dynamic load conditions.

The complex harmonics produced by the diode and thyristor nonlinear loads at various firing angles were effectively mitigated. The DC voltage stability was significantly improved throughout the operation of the shunt APF despite the introduction of sudden load change at time t = 0.4 s.

Table 3. Performance of the PR in (Amini et al., 2024) and the EPI - HOSM controllers during dynamic test

Description	**After compensation with SAPF**		
Controller type	PR controller Amini et al, 2024	EPI - HOSM control	Non-linear load
Total harmonic distortion %THD	3.38	2.05	
DC Voltage Stabilisation after load change	Unavailable	0.11 s	Diode RL
DC voltage overshoot	2 %	-	
DC voltage undershoot	2 %	-	
Power factor	< 0.99	< 0.99	

V. CONCLUSION

The growing number of nonlinear loads and renewable energy sources in electrical networks has amplified power quality challenges, necessitating advanced control techniques for effective harmonics mitigation in these networks. This study investigates the application of Higher-Order Sliding Mode (HOSM) control and Enhanced Proportional-Integral (EPI) controllers in Shunt Active Power Filters (SAPFs) to attain superior harmonic suppression and improved network stability. The combination of the EPI and HOSM ensures improved robustness against grid uncertainties and effective compensation under varying load conditions.

The simulation results confirm that the adopted EPI-HOSM technique significantly outperforms proportional resonant (PR) and conventional PI controllers in reducing Total Harmonic Distortion (THD) and improving dynamic response. The system achieves faster and lasting stability under fluctuating grid conditions, demonstrating its viability for real-world applications. The system achieved voltage stabilization within a short period, with stabilization occurring in just 0.1 seconds after the load change was introduced. The THD values in the two schemes were below the 5% limit set under the IEEE 519 regulations.

While the performance improvements are notable, challenges related to computational complexity, and real-time implementation constraints underscore the need for high-performance field programmable gate Arrays (FPGAs) or digital signal processors (DSPs).

Future studies can concentrate on hybrid control techniques, incorporating machine learning (ML) and artificial intelligence (AI) for self-tuning strategies to further enhance the efficiency of shunt APFs under dynamic load conditions. This study ultimately aims to contribute to the advancement of robust control strategies for power quality improvement, promoting the development of an efficient and sustainable grid infrastructure.

AUTHOR CONTRIBUTIONS

Z. G. Usman: Conceptualization, Methodology, Software, Validation, Writing – original draft. **O. Oghorada:** Conceptualization, Methodology, Supervision, Writing – review & editing. **O. Oshiga** and **B. Adetokun:** Supervision, Writing – review & editing.

REFERENCES

Ahmed, A. H., Kotb, A. E. S. B. and Ali, A. M. (2018). Comparison between Fuzzy Logic and PI Control for The Speed Of BLDC Motor. *International Journal of Power Electronics and Drive Systems (IJPEDS)*, 9(3), 1116.

Amini, B., Rastegar, H. and Pichan, M. (2024). An optimized proportional resonant current controller based genetic algorithm for enhancing shunt active power filter performance. *International Journal of Electrical Power & Energy Systems*, 156, 109738.

Bartolini, G., Ferrara, A. and Usai, E. (1998). Chattering avoidance by second-order sliding mode control. *IEEE Transactions on Automatic Control*, 43(2), 241–246.

Ben Abdelkader, A., Mouloudi, Y. and Amine Soumeur, M. (2023). Integration of renewable energy sources in the dynamic voltage restorer for improving power quality using ANFIS controller. *Journal of King Saud University - Engineering Sciences*, 35(8), 539–548.

Benbouhenni, H., (2019). Comparison study between SVPWM and FSVPWM strategy in fuzzy second order sliding mode control of a DFIG-based wind turbine. *Carpathian Journal of Electronic and Computer Engineering* 12(2), 1–10.

Buła, D., Grabowski, D. and Maciążek, M. (2022). A Review on Optimization of Active Power Filter Placement and Sizing Methods. *Energies*, 15(3), 1175.

Callegari, J.M.S., Cupertino, A.F., Ferreira, V.D.N. and Pereira, H.A., (2021). Minimum DC-Link Voltage Control for Efficiency and Reliability Improvement in PV Inverters. *IEEE Trans Power Electron*, 36(5), 5512–5520.

Cucuzzella, M., Incremona, G.P. and Ferrara, A., (2015). Design of Robust Higher Order Sliding Mode Control for Microgrids. *IEEE Journal on Emerging and Selected Topics in Circuits and Systems* 5(3), 393–401.

Deffaf, B., Farid, H., Benbouhenni, H., Medjmadj, S. and Debdouche, N. (2023). Synergetic control for three-level voltage source inverter-based shunt active power filter to improve power quality. *Energy Reports* 10, 1013–1027.

Divyalakshmi, D., and Subramaniam, N. P. (2017). Photovoltaic based DVR with Power Quality Detection using Wavelet Transform. *Energy Procedia*, 117, 458–465.

Donghua Chen and Shaojun Xie, (2004), Review of the control strategies applied to active power filters, *2004 IEEE International Conference on Electric Utility Deregulation, Restructuring and Power Technologies.* Proceedings, Hong Kong, China, pp. 666-670 Vol.2,

dos Santos Alonso, A. M., Brandao, D. I., Tedeschi, E., and Marafão, F. P. (2020). Distributed selective harmonic mitigation and decoupled unbalance compensation by coordinated inverters in three-phase four-wire low-voltage networks. *Electric Power Systems Research*, 186.

Hoon, Y., Mohd Radzi, M., Hassan, M., and Mailah, N. (2016). DC-Link Capacitor Voltage Regulation for Three-Phase Three-Level Inverter-Based Shunt Active Power Filter with Inverted Error Deviation Control. *Energies*, 9(7), 533.

Karafotis, P. A., Evangelopoulos, V. A., and Georgilakis, P. S. (2020). Evaluation of harmonic contribution to unbalance in power systems under non-stationary conditions using wavelet packet transform. *Electric Power Systems Research*, 178, 106026.

Komurcugil, H., Biricik, S., Bayhan, S., and Zhang, Z. (2021). Sliding Mode Control: Overview of Its Applications in Power Converters. *IEEE Industrial Electronics Magazine*, 15(1), 40–49.

Kumar, P. P., Sai, P., Sarat, S., and Sahu, K. (2015). Direct and Indirect current control of UPQC for enhancing power quality. *International Journal of Electrical and Electronics Engineering Research (IJEEER)*, 5(5), 93-106. www.tjprc.org

Li, D., Wang, T., Pan, W., Ding, X., and Gong, J. (2021). A comprehensive review of improving power quality using active power filters. *Electric Power Systems Research*, 199, 107389.

Musa, S., Radzi, M. A. M., Hisham, H., and Abdulwahab, N. I. (2014). Fuzzy logic controller-based three-phase shunt active power filter for harmonics reduction. *2014 IEEE Conference on Energy Conversion (CENCON)*, 371–376.

Musa, S., Radzi, M., Hizam, H., Wahab, N., Hoon, Y., and Zainuri, M. (2017). Modified Synchronous Reference Frame Based Shunt Active Power Filter with Fuzzy Logic Control Pulse Width Modulation Inverter. *Energies*, 10(6), 758.

Naftahi, K., Abouloifa, A., Hekss, Z., Echalih, S., Ait bellah, F., and Lachkar, I. (2022). Three-Phase Four-Wire

Shunt Active Power Filter Based on the Hybrid Automaton Control with Instantaneous Reactive Power Theory. *IFAC-PapersOnLine*, 55(12), 532–537.

Panda, A.K., and Patel, R., (2015). Adaptive hysteresis and fuzzy logic controlled-based shunt active power filter resistant to shoot-through phenomenon. *IET Power Electronics* 8(10), 1963–1977, https://doi.org/10.1049/iet-pel.2014.068

Rahman, N. A., Kamarudin, K., and Baharom, R. (2020). Boost Active Power Factor Correction Converter Using Various Current Controllers in Double Loop Control Algorithm. *2020 IEEE International Conference on Power and Energy (PECon)*, 24–28.

Sozanski, K., and Szczesniak, P. (2023). Advanced Control Algorithm for Three-Phase Shunt Active Power Filter Using Sliding DFT. *Energies*, 16(3).

Vargas-Gil, G. M., Colque, C. J. C., Sguarezi, A. J., and Monaro, R. M. (2017). Sliding mode plus PI control applied in PV systems control. *2017 IEEE 6th International Conference on Renewable Energy Research and Applications (ICRERA)*, 562–567.

Wang, Y., Wang, Y., Chen, S.-Z., Zhang, G., and Zhang, Y. (2018). A Simplified Minimum DC-Link Voltage Control Strategy for Shunt Active Power Filters. *Energies*, 11(9), 2407.

Wang, Y., Xie, Y., and Liu, X. (2015). The influence of DC-link voltage control on the performance of active power filter. *2015 IEEE Applied Power Electronics Conference and Exposition (APEC)*, 3183–3189.

Zafar, S., Amin, M. A., Javaid, B., and Khalid, H. A. (2018). On Design of DC-Link Voltage Controller and PQ Controller for Grid Connected VSC for Microgrid Application. *2018 International Conference on Power Generation Systems and Renewable Energy Technologies (PGSRET)*, 1–6.

Zenteno-Torres, J., Cieslak, J., Dávila, J., and Henry, D. (2021). Sliding Mode Control with Application to Fault-Tolerant Control: Assessment and Open Problems. *Automation*, 2(1), 1–30.